# SPATIO-TEMPORAL FLUCTUATIONS IN He I 10830 Å LINE PARAMETERS: EVIDENCE FOR SPICULE FORMATION

P. VENKATAKRISHNAN, S. K. JAIN, JAGDEV SINGH

*Indian Institute of Astrophysics, Bangalore 560034, India*

F. RECELY

*Space Environmental Laboratory, NOAA, Boulder, Colorado, U.S.A.*

and

W. C. LIVINGSTON

*National Solar Observatory, Tucson, U.S.A.*

(Received 5 February 1991; in revised form 13 July 1991)

**Abstract.** The equivalent width, line depth, line width, and Doppler shift of the He I 10830 Å line were extracted from two time series of spectra. Scatter plots of time-averaged line depth, line width, and Doppler shifts, as well as the root mean square temporal fluctuation of these quantities against the time-averaged equivalent width at a few hundred spatial locations were obtained. The statistical behaviour of these line parameters and their fluctuations was used to infer plausible reasons for the fluctuations. Examination of these results showed that the line parameter fluctuations could be caused by fluctuations in the coronal UV radiation (which could drive the spicules) or by the appearance of density inhomogeneities such as spicules within the line forming domain. In either case, the data can be interpreted as representing the initial phases of spicules.

## 1. Introduction

The He I 10830 Å line is an indicator of both coronal as well as chromospheric dynamics (De Jager, Namba, and Neeven, 1966; Milkey, Heasely, and Beebe, 1973; Harvey and Sheeley, 1977; Zirker, 1977; Venkatakrishnan and Jain, 1983). The coronal signature arises due to the excitation of the helium atom to its 3S (19.6 eV) state by back radiation from coronal UV lines (e.g., He II 304 Å). Thus changes in the coronal UV intensities would be expected to be manifested as changes in the amount of He I 10830 Å absorption. The chromospheric signature could possibly arise due to an increase in the number of absorbing atoms in the line of sight either by a change in the plasma density (in quiet conditions) or by collisional excitation caused by enhancement of temperature (during activity).

Observations in the He I 10830 Å line by Giovanelli and Hall (1977) with a resolution of 2 arc sec reveal that the line depth over supergranular cell centres ($\sim 0.021$) is smaller than over the network boundary ($\sim 0.075$). If one assumes that the network centre is devoid of spicules and the boundary is filled with them, then one can attribute the increase in line depth to a larger number of spicules (Zirin, 1966). It is interesting to note that De Jager, Namba, and Neeven (1966) have identified the helium mottles with spicules.

*Solar Physics* **138:** 107–121, 1992.

Spicules are, however, transient structures (Kulidzhanishvili and Nikolsky, 1978) with a lifetime of $\approx 5$ min. Thus, monitoring of the profiles of the He I 10830 Å line as a function of time will reveal interesting details of a spicule's life history. Since spicules undergo changes in their density, flow velocity, and temperature characteristics during their life times, it is imperative that one monitor all the parameters of the line, viz., its depth, equivalent width, line shift, and line width. By studying the time variation of these parameters, one can obtain important clues to the origin and dynamics of spicules. With this objective in mind, we obtained a series of He I 10830 Å spectra every minute along a line of 512 spatial locations on the Sun for a total duration of $3\frac{1}{2}$ hours on 20 January 1985 and for a duration of 72 min on 2 June, 1986. In this paper we treat the individual pixels as statistically independent entities and examine the relationships of the time-averaged line depth, line width, and line shift, with the time-averaged equivalent width by means of scatter diagrams. We also study the temporal variance of the fluctuation of the line parameters as a function of the mean equivalent width. We describe the observations and data reduction in Section 2, results in Section 3 and the implications of these results in Section 4.

## 2. Observations and Data Reduction

The spectra were obtained using the vacuum tower telescope and the 512 channel magnetograph of the National Solar Observatory at Kitt Peak (Livingston *et al.*, 1976). The magnetograph consists of two arrays of 512 diodes each. In this experiment, only one array was used. The pixel size corresponding to each diode is 1 arc sec$^2$. Seeing conditions were fair ($\approx 2$ arc sec). To obtain the spectra, the solar image was kept fixed with the entrance slit aligned E–W over a position close to disc center. The diode array was then scanned in wavelength to record the spectrum over 70 channels, each 0.14 Å wide.

Observations were taken in the following sequence. First, a spectroheliogram in He I 10830 Å line was obtained to identify the slit position on the solar surface. Then sixty spectra in the wavelength range of $\lambda\lambda$10825 Å to 10835 Å were obtained at a rate of one per minute. Again, a spectroheliogram in the He I 10830 Å line was recorded to verify the slit position on the solar surface. A comparison of the two spectroheliograms showed that the position of the slit was still properly aligned in the E–W direction. This sequence of recording spectra and spectroheliograms was followed subsequently. Thus, three batches of spectra (two of 60 min and one of 30 min duration), and four spectroheliograms were recorded on 20 January, 1985. A similar procedure was followed on 2 June, 1986 as well. The temporal interval, however, was 30 s on 2 June, 1986 as against 60 s on 20 January 1985.

The data, recorded on 9 track tapes, were reduced at the VAX 11/780 computer at Kavalur. The spectrograph slit covered 512 arc sec on the Sun in the east–west direction. Owing to the rotation of the Sun, features on the solar surface move from east to west at the rate of 1 arc sec ($\equiv$ 1 pixel) every 6 min. To track the same location on the solar surface, successively westward pixels were considered after every 6 min during

the analysis. Thus, after correcting for solar rotation, data for only 500 arc sec were left in the observing window.

Further, since the 'seeing' was only 2 arc sec, spectra of two neighbouring pixels were combined. Thus, we were left with spectra at 250 spatial locations, each location being $2 \times 1$ arc sec$^2$, for the first batch of spectra of 60 min duration. Similar procedures were followed for the other batches of spectra. These sets of spectra were used for the subsequent analysis, such as computation of equivalent widths, etc.

## 3. Results

For illustration purposes, we show in Figure 1 two representative spectra at two different times (separated by 9 min), obtained at the same location. Similarly, in Figure 2 we show time-averaged spectra at four different locations. Marked differences are seen in the line profiles in both of the cases, showing variation in space as well as in time.

Spectroheliograms of the observed solar region obtained in the He I 10830 Å line are shown in Figure 3. In all these pictures the supergranular pattern is seen quite well. Each cell boundary is made up of a few well-defined patches having sizes $\leq 10$ arc sec. Such a structure is well known in Ca K and H$\alpha$ pictures where these are called flocculus and rosette, respectively. The appearance of the solar disc in the He I 10830 Å line is already well known and extensively discussed in the literature. In this paper, we will use the simultaneous temporal variation of the line parameters as a diagnostic of a possible origin for these structures in He I 10830 Å.

The line parameters were determined in the following manner. The equivalent width was measured as the area under the profile, keeping the reference continuum level as the mean of four intensity values at $\lambda\lambda$10829.09 Å, 10829.23 Å, 10829.37 Å, and 10829.51 Å, respectively. All these points lie on the violet side of the line. We deliberately avoided the red side of the line since large fluctuations in the continuum intensity were noticed on this side. Because the contribution of the wings to equivalent width is extremely small, we expect no significant changes in the equivalent width caused directly by such fluctuations in the far wings. This expectation was borne out *a posteriori* in the relationship between equivalent width and line depth, as will be seen later.

The centroid of the line was determined for estimating the line shifts. To identify the centroid, we started with a point on the red wing of the line and moved towards smaller wavelengths, performing a running integration of the residual intensity over wavelength. The integration was stopped wherever the integral exceeded half the equivalent width, and the centroid was calculated by interpolating between the current and previous values of the wavelength. We realise now that this centroid could be biased by less than 0.5 km s$^{-1}$ towards redward values for more intense profiles, since the red wing fluctuations are more pronounced for intense profiles (Figures 1 and 2). We will refer to this again at a suitable place. The deviation of this centroid from an arbitrary zero-velocity position (corresponding to the laboratory value of the line centre) was used to convert the line shift into velocity units. Redward deviations were assumed positive. The line depth calculations will be influenced only marginally by the fluctuations in the line wings.

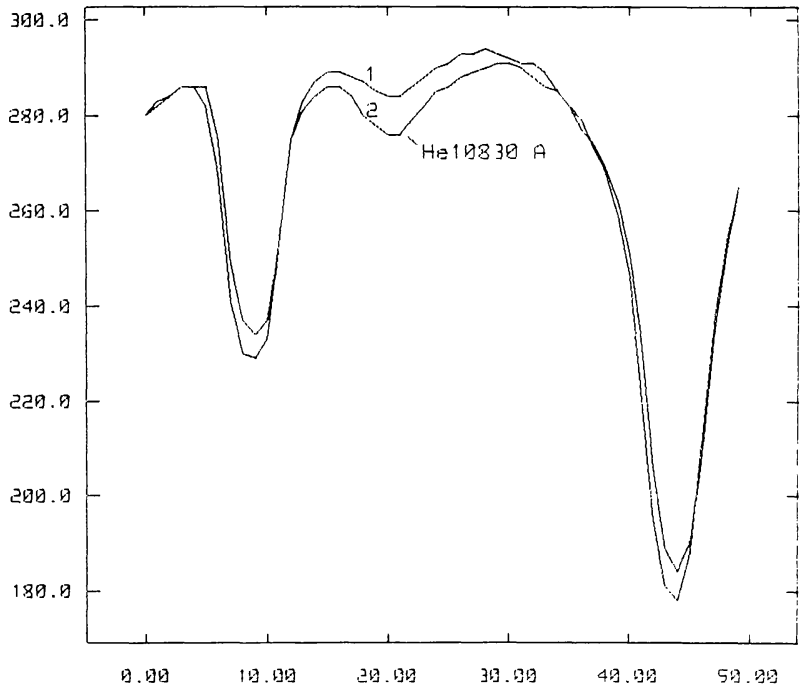


Fig. 1. Spectra in the region of He I 10830 Å line obtained at two different times (marked 1 and 2) separated by 9 minutes, at the same location. Wavelength decreases towards right.

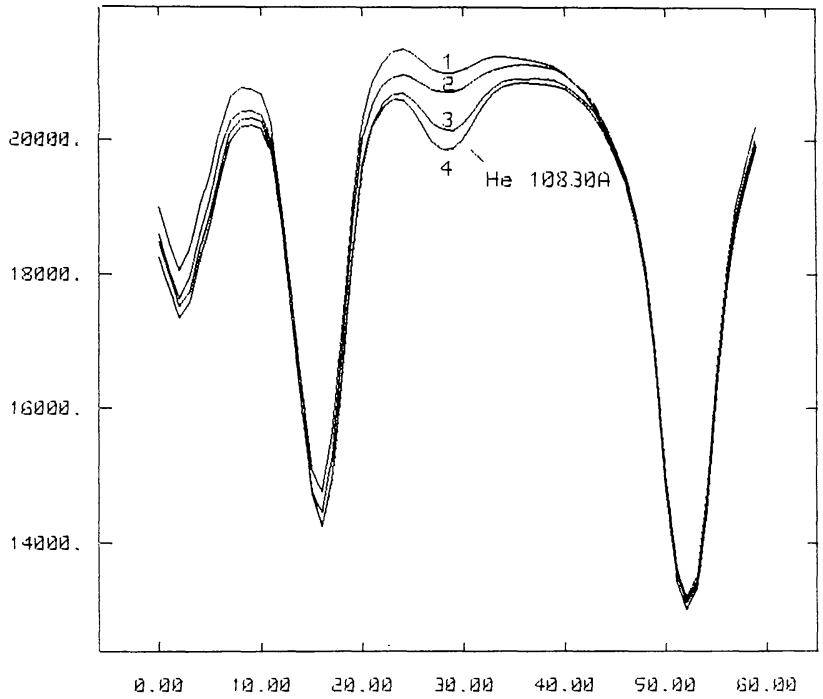


Fig. 2. Time-averaged spectra at four different locations along the slit. The labels 1, 2, 3, and 4 represent the profiles with equivalent widths of 9, 16, 42, and 66 mÅ, respectively.

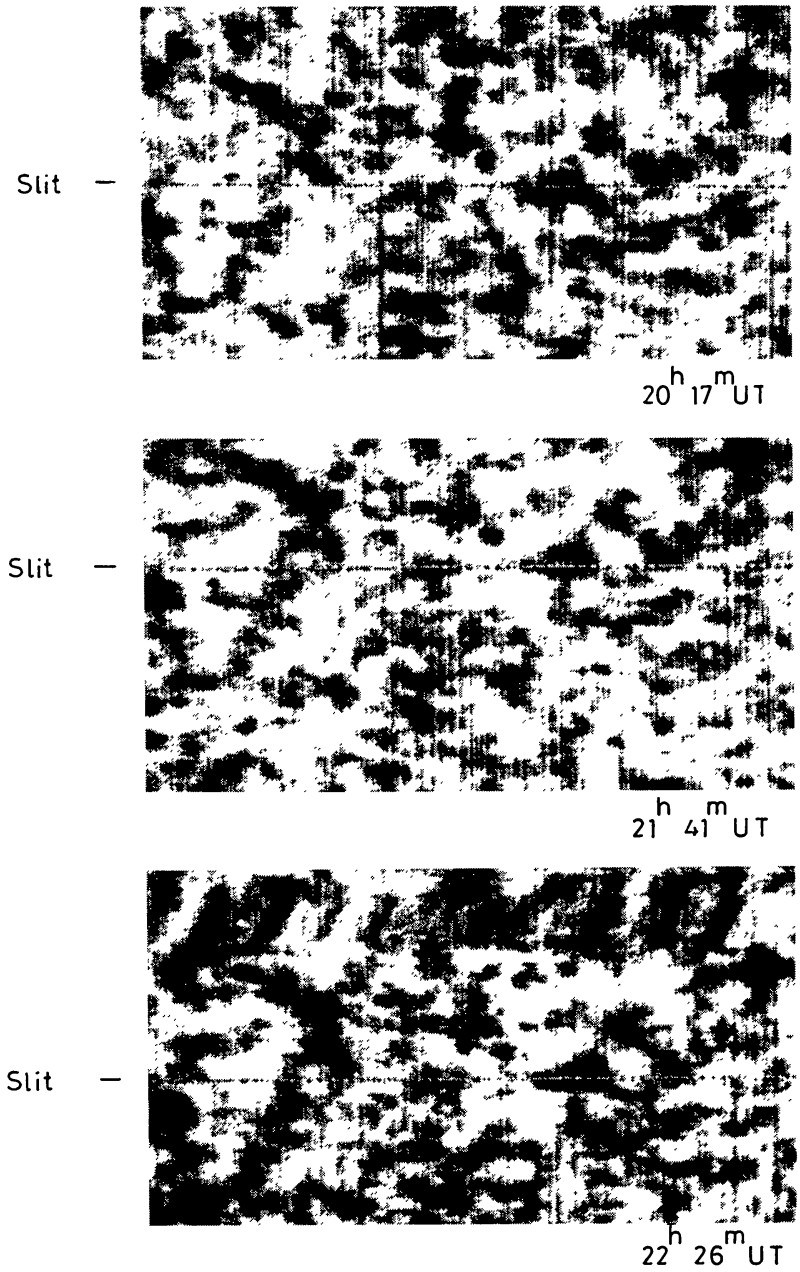


Fig. 3. Spectroheliograms obtained during the 20 January, 1985 run. The position of the entrance slit of the spectrograph is seen as a horizontal line.

Likewise, the line width is defined as the full width at half maximum and thus is not expected to be influenced by the wing intensity fluctuations.

To understand the time independent properties of the line, all these parameters were averaged in time at each of the 250 pixels. Figures 4(a–c) show the scatter plot of the time-averaged equivalent width versus the mean line depth, line width, and velocity respectively, for the data obtained on 20 January, 1985. Figures 5(a–c) likewise show similar scatter plots for the data of 2 June, 1986. The striking similarity of the nature of the scatter for data on both the days adds credence to the generality of any conclusions that we might draw from these plots.

The range of the abscissae, viz., equivalent width, is quite large. We have values as low as 0.005 Å to as high as 0.04 Å on both days. There seem to be a few more extreme values of equivalent width on 2 June.

The tight correlation of line depth with the equivalent width shows that most of the

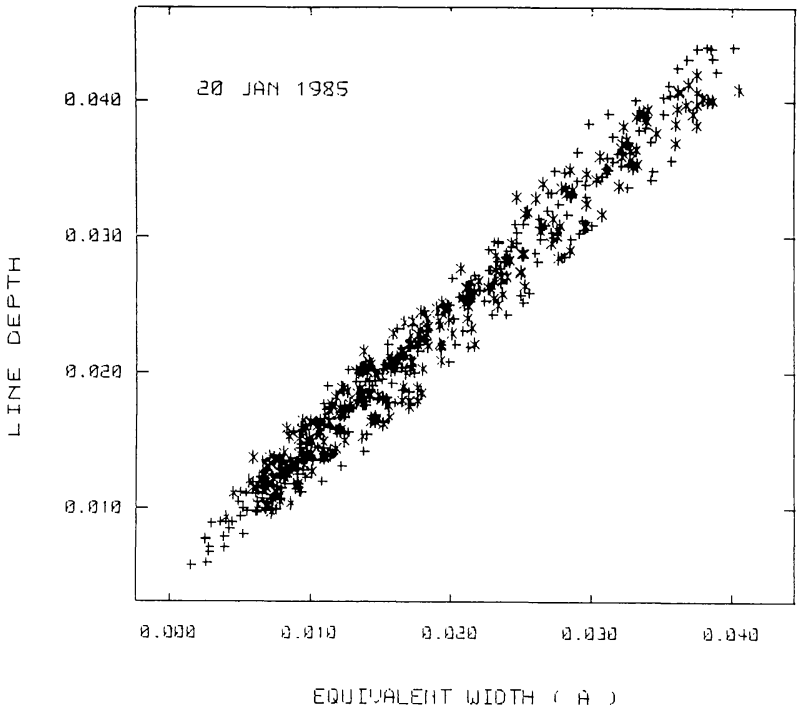


Fig. 4a.

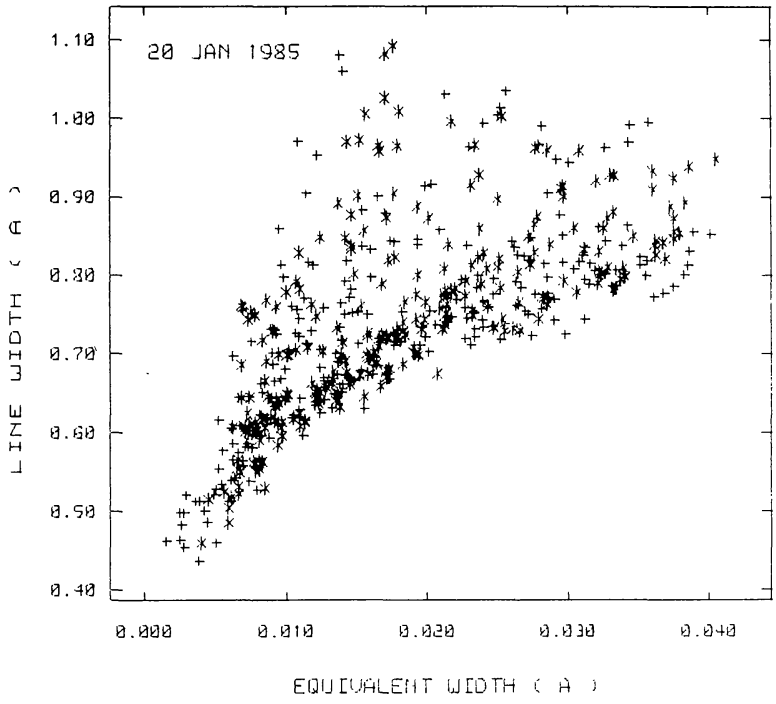


Fig. 4b.

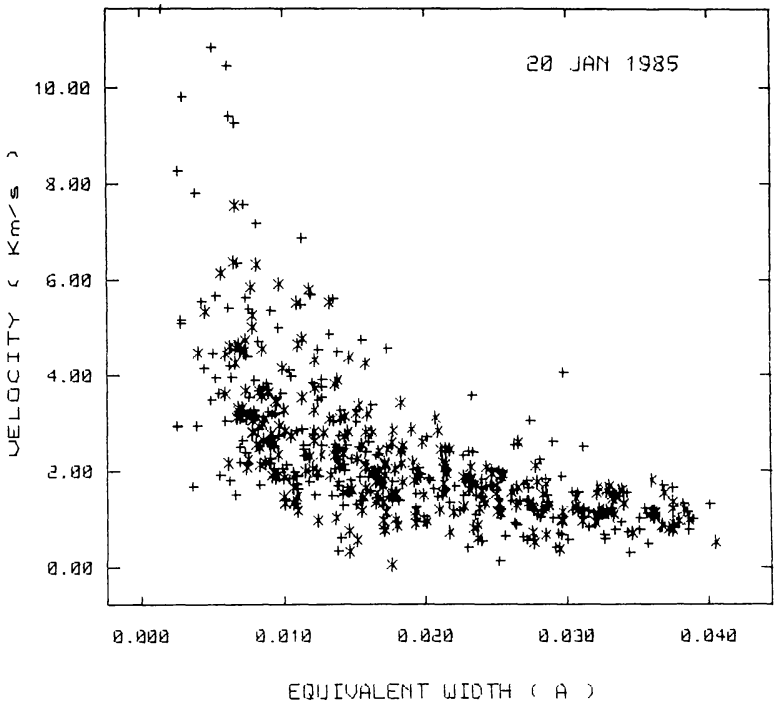


Fig. 4c.

Fig. 4. Scatter plots of time-averaged equivalent width versus time-averaged (a) line depth, (b) line width, and (c) velocity, for data obtained on 20 January, 1985.

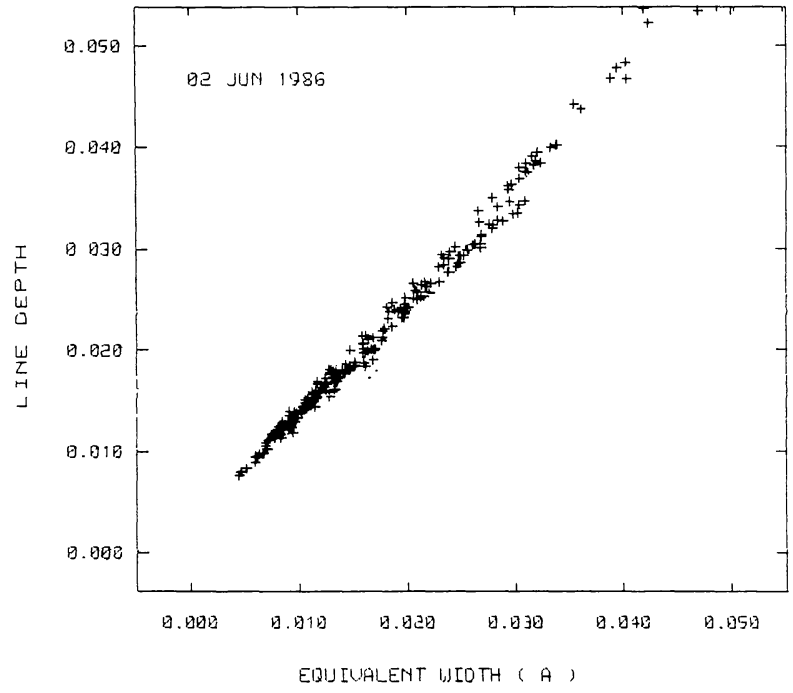


Fig. 5a.

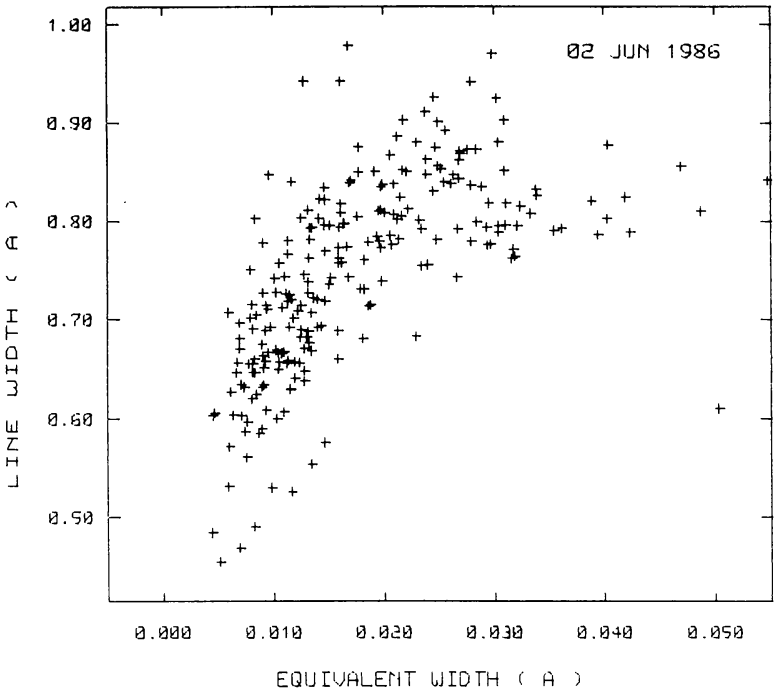


Fig. 5b.

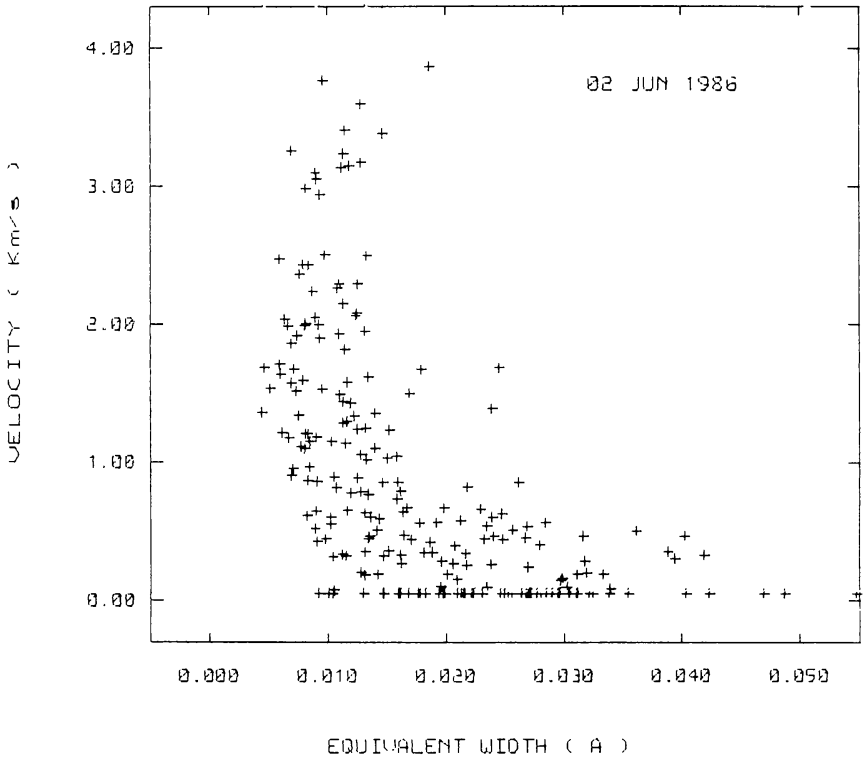


Fig. 5c.

Fig. 5. Same as in Figure 4 for data obtained on 2 June, 1986.

contribution to the equivalent width comes from a narrow region of the line profile near the line minimum. It also demonstrates that the line wing fluctuations had a negligible effect on the equivalent width calculations.

We now come to the line width vs equivalent width correlation. Figures 4(b) and 5(b) show a trend of increasing line width with equivalent width. The extreme value of the line width, viz., 1 Å, indicates a maximum temperature of 63 000 K. In comparison, the equivalent temperature for the 19 eV energy difference (between the lowest energy state of the singlet series for He to the lower energy state of the 10830 Å transition) is $2.2 \times 10^5$ K, which clearly rules out collisional excitation of the line. On the other hand, the temperature of spicules is in the range of 6000 K for a wide range of heights (Beckers, 1968), although Zirin (1989) does not confirm this. If the material associated with the large equivalent width has a low temperature, then a significant fraction of the observed line width must have a kinematic origin.

The trend of lower velocity for larger equivalent width (Figures 4(c) and 5(c)) is perhaps real, bearing in mind that the increased red wing depressions for stronger profiles would have resulted in an opposite trend. Assuming that the observed trend is real, one can conclude that the regions of large equivalent width are relatively blue shifted with respect to the regions of lower equivalent width.

Having looked at the time averaged line parameters, let us now consider the temporal fluctuations of these parameters. A very good measure of the total power in these fluctuations is the variance or, alternatively, the root mean square deviation of the parameters from their mean values.

Figures 6(a–d) show the scatter plots of the r.m.s. equivalent width, line depth, line width, and velocity as a function of the mean equivalent width for the 20 January data. Similarly Figures 7(a–d) are the plots for the 2 June data.

Before describing the results of Figures 6 and 7, let us digress for a moment to understand the cause of the spatial variation of the mean equivalent width. We offer two plausible reasons. One reason could be the variation of the number density of smaller structures seen within the observing aperture, generally referred to as the 'filling factor'. The other could be a straightforward variation in the column density of absorbing atoms over the pixel.

Figures 6(a) and 7(a) show an increase in the r.m.s equivalent width as a function of mean equivalent width. This trend of increasing fluctuations with increasing mean equivalent width can be reconciled in the 'filling factor' model, only if the fluctuations of the smaller structures are coherent over the spatial scale of the pixel. On the other hand, the trend of increasing fluctuations with increasing mean equivalent width points to a non-Gaussian distribution of events in the column density interpretation of the variations mentioned above. In either case the trend indicates a real solar phenomenon. The same trend is seen in the fluctuations in line depth (Figures 6(b) and 7(b)). However, Figures 6(c) and 7(c) show decreasing r.m.s. line width fluctuations with mean equivalent width. The temporal fluctuations of the line width are not above $\approx 0.2$ Å for strong line profiles. If the line width is kinematically produced, then this indicates a 20% fluctuation of the turbulence strength within a fraction of the total observed time. Once

again, if one considers spicules, then the sound travel time over the height of the spicules will itself be $\approx 1000$ s and thus very rapid fluctuations in the turbulence strength seem highly unlikely. On the other hand the temperature fluctuation corresponding to 0.2 Å is 2500 K (temperature $T = 6.32 \times 10^4 \times$ (FWHM in Å)$^2$ for He atom). This is 40% of 6000 K, the generally accepted temperature of spicules.

Likewise, Figures 6(d) and 7(d) show decreasing r.m.s. velocity fluctuations with increasing mean equivalent width. The low value of 2 km s$^{-1}$ for the fluctuations in the regions of large mean equivalent width once again rules out the existence of large motions in these regions.

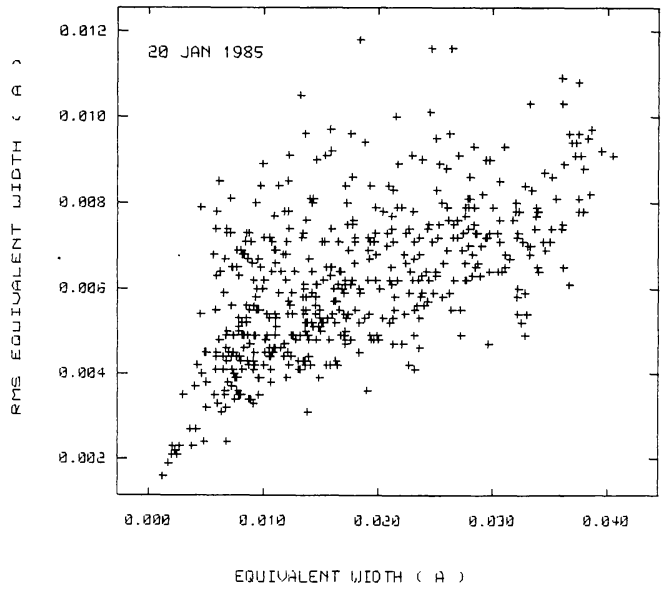


Fig. 6a.

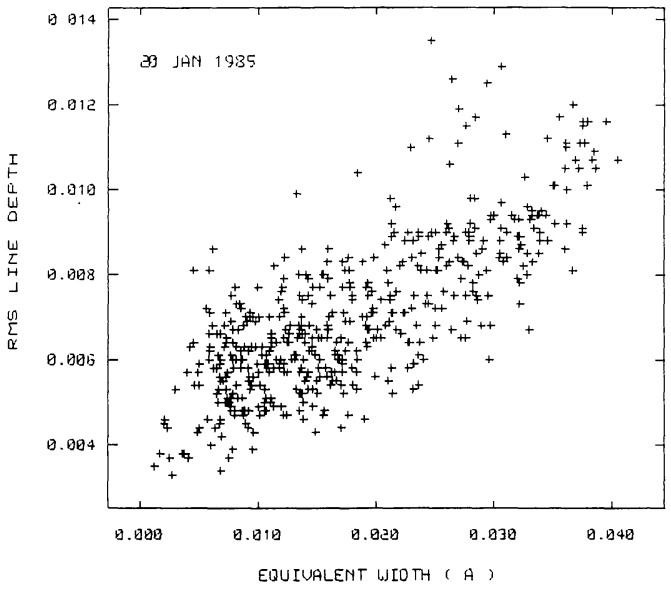


Fig. 6b.

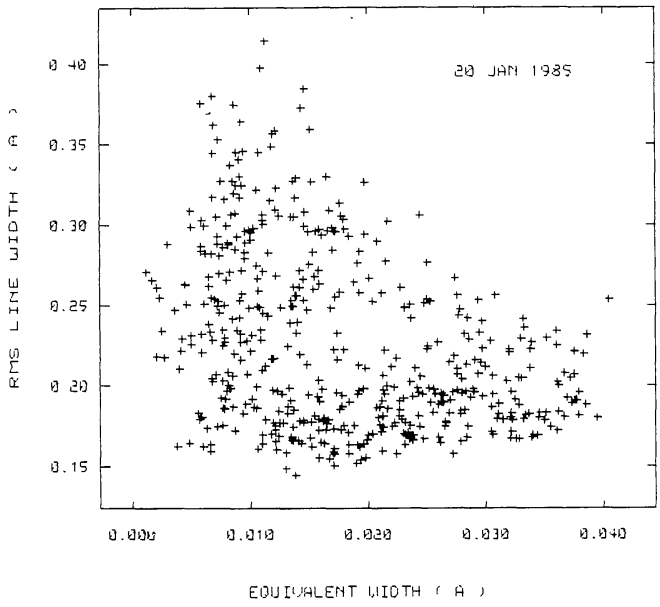


Fig. 6c.

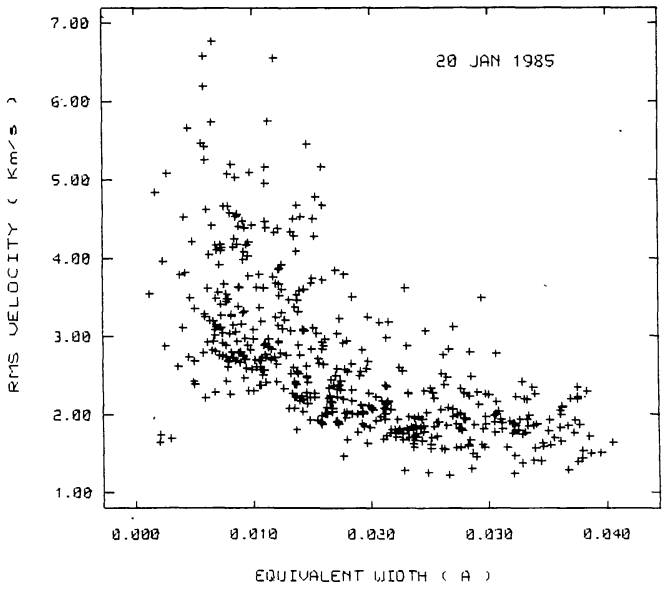


Fig. 6d.

Fig. 6. Scatter plots of time-averaged equivalent width versus the r.m.s. temporal fluctuation in (a) equivalent width, (b) line depth, (c) line width, and (d) velocity, for the 20 January, 1985 data.

## 4. Discussion and Conclusions

Observations of a single line are not sufficient to model the cause of the line variations uniquely. Nontheless, certain basic information can be extracted from the results presented in the previous section.

The trend of increasing line width with equivalent width for the time averaged data provides an important clue about the material at the locations of large equivalent width.

First of all, an increase in equivalent width – viz., an increase in the number of absorbing atoms in the line of sight – can be caused either by an increase in the plasma density or by an increase in the excitation rate. An increase in plasma density, coupled with an increase in temperature or turbulence (see Figures 4(b) and 5(b)), results in a pressure enhancement. This high-pressure plasma cannot be confined by the external plasma with a lower pressure. The spatial correspondence of the darker He I structure with the chromospheric network implies a stronger magnetic field in these high pressure locations, ruling out the confinement of the gas by external magnetic pressure. Confinement is implied because the time scale of pressure expansion over the size of the pixel (2″)

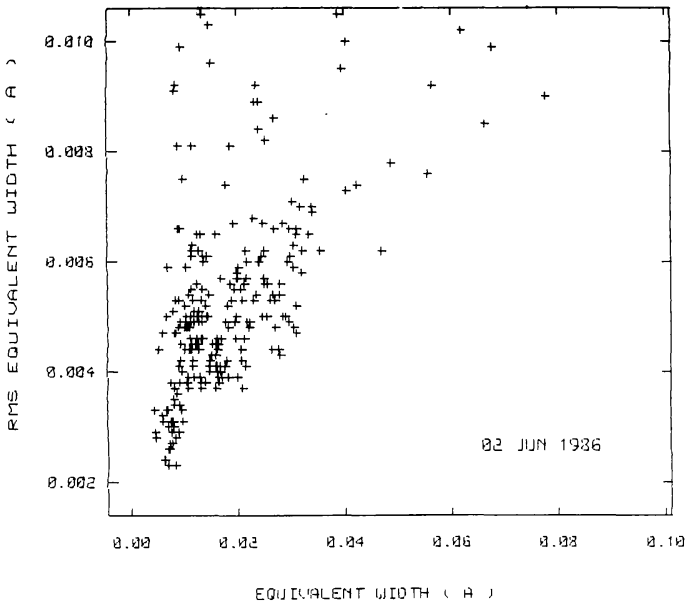


Fig. 7a.

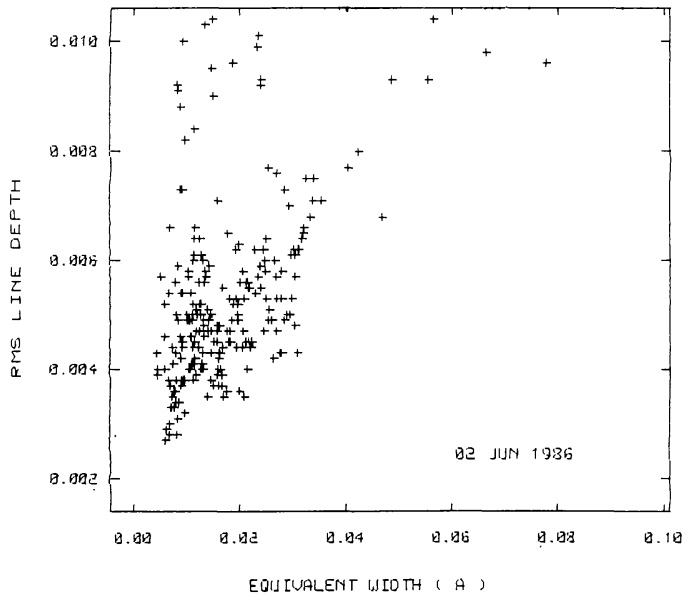


Fig. 7b.

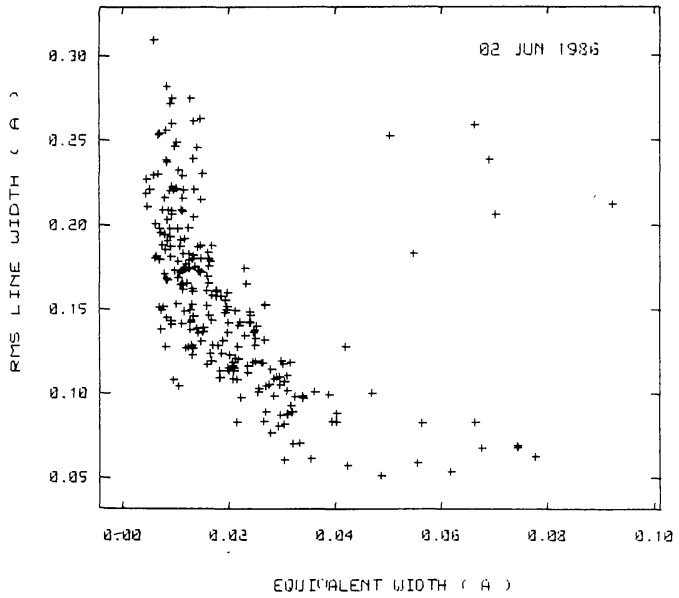


Fig. 7c.

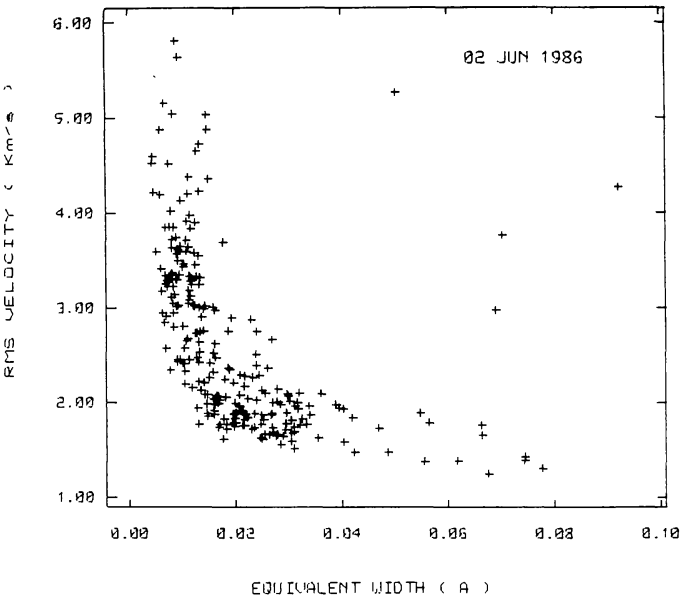


Fig. 7d.

Fig. 7. Same as in Figure 6 for the 2 June, 1986 data.

is $\approx 150$ s for a sound speed of 10 km s$^{-1}$, whereas the time average is taken over a much larger interval of $\approx 60$ min. Thus, the interpretation of the time-averaged excess equivalent width at certain locations in terms of density inhomogeneities is ruled out.

Hence, we can only conclude that the increase in equivalent width is caused by an increase in the excitation rate. The line width data rule out collisional excitation since the inferred temperatures fall short of the excitation temperature of the HeI 10830 Å line. Thus the increase in equivalent width must be due to an increase in the back

radiation from the transition region and corona. This is consistent with the spatial correlation of He II 304 Å and He I 10830 Å structures found by Harvey and Sheeley (1977). The trend of blue shifted profiles for larger equivalent widths (Figures 4(c) and 5(c)) is another significant result. If the trend were to be non-existent, then one would expect an equal number of data points on either side of a 'mean' velocity. The lopsided nature of the scatter plot is an indication of the reality of the trend. Physically, this trend can be interpreted in terms of a 'fountain' effect with matter rising in the regions of strong line profiles and descending in the regions of weaker profiles. The trend of increasing r.m.s. equivalent width fluctuations with increasing mean equivalent width (Figures 6(a) and 7(a)) is indicative of a real solar phenomenon as mentioned in Section 3. The interpretation of these fluctuations as due to fluctuations in the coronal/transition region UV intensity fluctuations is, however, not explicit. One can also have the possibility of density inhomogeneities erupting into the line formation domain of He I 10830 Å, getting excited by the coronal UV radiation, and thereby increasing the equivalent width. Spicules can possibly do this. However, since the velocity fluctuations are small ($\approx 2$ km s$^{-1}$), we are probably looking only at the roots of the spicules with most of the acceleration to 20 km s$^{-1}$ occurring above the formation depth of the He I 10830 Å line. The actual amount of material involved in this process need not be very large since the r.m.s. fluctuation of the equivalent width is only 20% of the mean for the stronger profiles.

The alternative interpretation, viz., fluctuations in UV radiation causing the equivalent width fluctuations, would require an accompanying fluctuation of temperature caused by the fluctuating ionisation and heating of the material. The resulting 'chromospheric evaporation' can then be identified with spicules. The r.m.s. line width fluctuations, however, show a smaller value at larger values of mean equivalent width (Figures 6(c) and 7(c)). This does not completely rule out the second interpretation since the large scatter at low equivalent width could be explained as due to poor signal to noise in the line width determination. Data obtained with a better spectral resolution can perhaps settle the issue. Incidentally, the r.m.s. velocity fluctuation also shows a decreasing trend for stronger profiles which can once again be interpreted as due to poor signal to noise in the weaker profiles.

If at all the fluctuating equivalent width is due to a fluctuating coronal UV component, then one could identify these fluctuations with a number of observed phenomena, e.g., UV jets (Dere, 1985), microflares (Porter *et al.*, 1986), or nanoflares (Parker, 1987). Theoretically, these fluctuations would seem to result from reconnections produced from the constant twisting and braiding motions of the photospheric foot points of the magnetic field lines (Parker, 1987; van Ballegooijen, 1985). It would be very satisfying to unify the phenomena such as spicules, macro-spicules, jets and microflares into a single hydrodynamical model in the future.

To summarise, what we have essentially shown in this paper is evidence for coronal/transition region UV back radiation as the cause for the time-averaged spatial fluctuations in He I 10830 Å line parameters. The temporal fluctuations could either be due to spicules erupting into the He I 10830 Å line formation region, or be due to

fluctuations in the coronal UV radiation. The excess transient heating caused by the latter could possibly lead to spicules by 'chromospheric evaporation'. In either case, the low value of the velocity fluctuations suggests that we are looking at the 'roots' of the spicule phenomenon with the acceleration to spicular velocities occurring above the line formation height.

## Acknowledgements

It is a pleasure to thank Mr V. Chandramouli who worked for Computer Maintenance Corporation of India, for his help in reading the KPNO magnetic tapes. The visit of J.S. to KPNO was financed by the Director, National Solar Observatory, National Optical Astronomical Observatories, operated by the Association of Universities for Research in Astronomy, Inc., under contract with the National Science Foundation. A travel grant to J.S. was provided by NSF.

## References

Beckers, J. M.: 1968, *Solar Phys.* **3**, 367.
De Jager, C., Namba, O., and Neeven, L.: 1966, *Bull. Astron. Inst. Neth.* **18**, 128.
Giovanelli, R. G. and Hall, D.: 1977, *Solar Phys.* **52**, 211.
Harvey, J. W. and Sheeley, N. R., Jr.: 1977, *Solar Phys.* **54**, 343.
Kulidzhanishvili, V. I. and Nikolsky, G. M.: 1978, *Solar Phys.* **59**, 1.
Livingston, W. C., Harvey, J. W., Slaughter, C. D., and Trumbo, D.: 1976, *Appl. Opt.* **15**, 40.
Milkey, R. W., Heasley, J. N., and Beebe, H. A.: 1973, *Astrophys. J.* **186**, 1043.
Parker, E. N.: 1987, in G. Athay and D. S. Spicer (eds.), *Theoretical Problems in High Resolution Solar Physics II*, NASA CP 2483, p. 89.
Porter, J. G., Reichmann, E. J., Moore, R. L., and Harvey, K. L.: 1986, in A. I. Poland (ed), *Coronal and Prominence Plasmas*, NASA CP 2442, p. 383.
van Ballegooijen, A. A.: 1985, in H. U. Schmidt (ed.), *Theoretical Problems in High Resolution Solar Physics*, MPA 212, p. 268.
Venkatakrishnan, P. and Jain, S. K.: 1983, *Bull. Astron. Soc. India* **11**, 369.
Zirin, H.: 1966, *The Solar Atmosphere*, Blaisdell Publ. Co., Waltham, Massachusetts, p. 256.
Zirin, H.: 1989, *Astrophysics of the Sun*, Cambridge University Press, Cambridge, p. 176.
Zirker, J. B. (ed.): 1977, *Coronal Holes and High Speed Wind Streams*, Colorado Associated University Press, Bouler.